Realization of large transmitted Goos–Hänchen shifts with high (near 100%) transmittance based on a coupled double-layer grating system

Shihao Du,[1] Zhiyuan Che,[1,*] Maoxiong Zhao,[1] Wenzhe Liu,[2] and Lei Shi[1,3,4] (iD)

[1] *State Key Laboratory of Surface Physics, Key Laboratory of Micro- and Nano-Photonic Structures (Ministry of Education) and Department of Physics, Fudan University, Shanghai 200433, China*
[2] *Department of Physics, The Hong Kong University of Science and Technology, Clear Water Bay, Kowloon, Hong Kong, China*
[3] *Institute for Nanoelectronic Devices and Quantum Computing, Fudan University, Shanghai 200438, China*
[4] *Collaborative Innovation Center of Advanced Microstructures, Nanjing University, Nanjing 210093, China*
Corresponding author: chezy@fudan.edu.cn

Achieving Goos–Hänchen shift enhancement with high transmittance or reflectance based on the resonance effect is challenging due to the drop in the resonance region. This Letter demonstrates the realization of large transmitted Goos–Hänchen shifts with high (near 100%) transmittance based on a coupled double-layer grating system. The double-layer grating is composed of two parallel and misaligned subwavelength dielectric gratings. By changing the distance and the relative dislocation between the two dielectric gratings, the coupling of the double-layer grating can be flexibly tuned. The transmittance of the double-layer grating can be close to 1 in the entire resonance angle region, and the gradient of the transmissive phase is also preserved. The Goos–Hänchen shift of the double-layer grating reaches ~30 times the wavelength, approaching 1.3 times the radius of the beam waist, which can be observed directly. © 2023 Optica Publishing Group

When a light beam hits the interface between two different media, it may undergo a lateral shift from the predictions of geometrical optics in the plane of incidence. This shift was first observed experimentally by Goos and Hänchen in 1947 and is called the Goos–Hänchen (GH) shift [1]. According to the stationary phase method proposed by Artmann [2], the GH shift is proportional to the partial derivative of the reflection phase to the incident angle. It is also applicable to transmitted light [3]. The GH shift has attracted much attention due to its exciting physics and potential applications in many fields, such as optical information storage [4], optical switches [5,6], beam splitters [7], and a variety of sensors [8–10].

The GH shift was studied in total internal reflection at the beginning [1]. In such cases, the GH shift is only a few times the wavelength, which poses a challenge in the experimental measurement. Therefore, the enlargement of the GH shift is essential. A common mechanism to enlarge GH shifts is to use the optical resonance effect. Due to the existence of a resonance, the reflective or transmissive phase changes drastically with the incident angle near the resonance angle, and the GH shift can be significantly enlarged [11,12]. According to this physical mechanism, various resonant microstructures have been proposed to enlarge the GH shift, including a weakly absorbing slab [13], epsilon-near-zero metamaterial slab [14], asymmetric double prism [15], compound grating waveguide structure [16,17], and photonic crystal (PhC) slabs [18–21]. However, there is a shortcoming: the transmitted GH shift is usually of low efficiency due to the maximum GH shift located at the transmittance dip where the transmittance is close to 0. This will cause the intensity of the shifted beam component to be very fragile, which is not conducive to various applications based on the GH shift. Furthermore, the resonance angle range is relatively narrow. It is not suitable for large-angle range incidents. Therefore, the GH shifts are far smaller than the beam waist, which is hard to observe directly in the experiment.

This paper proposes a coupled double-layer grating system (one-dimensional PhC slabs) to enhance the transmitted GH shift. By adjusting the distance and the relative dislocation between the upper grating and the lower grating, the coupling between gratings can be modulated to achieve high transmittance in the resonance angle region with drastic transmissive phase modulation. The modulation efficiency, which is the proportion of the shifted beam to the incident beam, has been significantly improved, and almost all the incoming power is modulated. Moreover, the magnitude of the GH shift is enhanced simultaneously. The GH shift reaches ~30 times the wavelength, approaching 1.3 times the radius of the beam waist, which can be observed directly. We use the rigorous coupled-wave analysis method to calculate the transmittance spectra and the relationship between the transmissive phase and incident angle [22]. The electric field distributions of the GH shift are obtained with the finite-difference time-domain method.

We have recently revealed that large transmitted optical GH shifts can be realized in a single-layer grating [21]. The transmitted resonance mode of the grating is chosen to enhance the GH shift, as shown in Fig. 1(a). The radiative modes of the grating can be excited by the incident light in free space, generating Fano resonances. Moreover, there would typically be a sharp phase
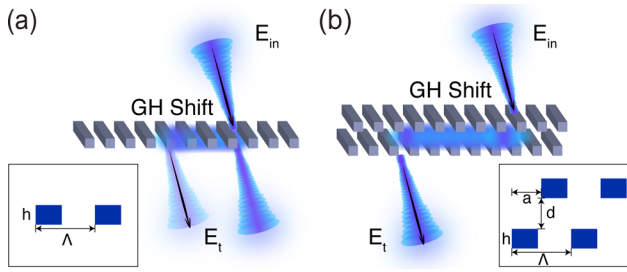
Fig. 1. Transmitted optical GH shift diagram of (a) the single grating and (b) the coupled double-layer grating system. The grating constant is denoted by Λ, and the height is denoted by h. The distance and the relative dislocation between two identical gratings are denoted by d and a, respectively.

change in Fano resonance, which could be used to enhance the GH shift [16,17]. The incident light field is usually a Gaussian beam. The transmitted GH shift of such a beam is the average of the shifts of the plane wave Gaussian beam components [23]:

$$\mathrm{GHS} = \frac{1}{T} \int G(k_x) \cdot t(k_x) \cdot \left(-\frac{\partial \phi_t}{\partial k_x}\right) dk_x, \qquad (1)$$

where G is the amplitude of the Gaussian wave packet, t is transmittance, ϕ_t is the transmissive phase, k_x is the magnitude of the component of the wave vector parallel to the surface, and T is the normalizing constant. However, there is a transmission dip in the resonance region of the transmissive phase change, rendering very low transmittance and low efficiency [21]. The GH shift becomes inefficient, which limits its practical applications.

To increase the efficiency of the GH shift, we design a coupled double-layer grating system formed by two identical sub-wavelength stacked and misaligned dielectric gratings in parallel. The coupling between the upper and lower gratings can be tuned to improve the transmittance while preserving the transmissive phase gradient. The coupling of the double-layer gratings can be adjusted through two degrees of freedom: the distance d, and the relative dislocation a between the upper grating and the lower grating. By optimizing d and a, it can be realized that the transmittance of the double-layer gratings is close to 1 in the resonance angle region and the phase gradient becomes twice that of the single-layer grating. The efficiency has improved and the GH shift has also become more significant, as shown in Fig. 1(b).

The effect of modulating distance d without dislocation is primarily considered on the transmittance spectrum and transmissive phase. The grating's refractive index is 2, while the background refractive index is set to 1.5. The grating thickness is chosen to be 150 nm, and the grating constant Λ is 500 nm. The filling fraction of the grating is 0.4. Figure 2(a) shows the calculated TE transmittance spectra for the single-layer grating. Figure 2(b) shows the angular spectra with transmittance and corresponding phase at $\lambda = 850$ nm, and the blue dashed line represents the wavelength in Fig. 2(a). In the resonance angle range, the transmitted beam has a drastic transmissive phase change, and the transmittance first drops to 0 at $\theta = 6.25°$ and then rises. Considering the coupled double-layer grating system with large modulating distance d, the calculated TE transmittance spectra and the angular spectra with transmittance and transmissive phase are shown in Figs. 2(c) and 2(d) for $d = 2.0 \, \mu\mathrm{m}$ (4.0Λ). It can be seen that there is slight coupling
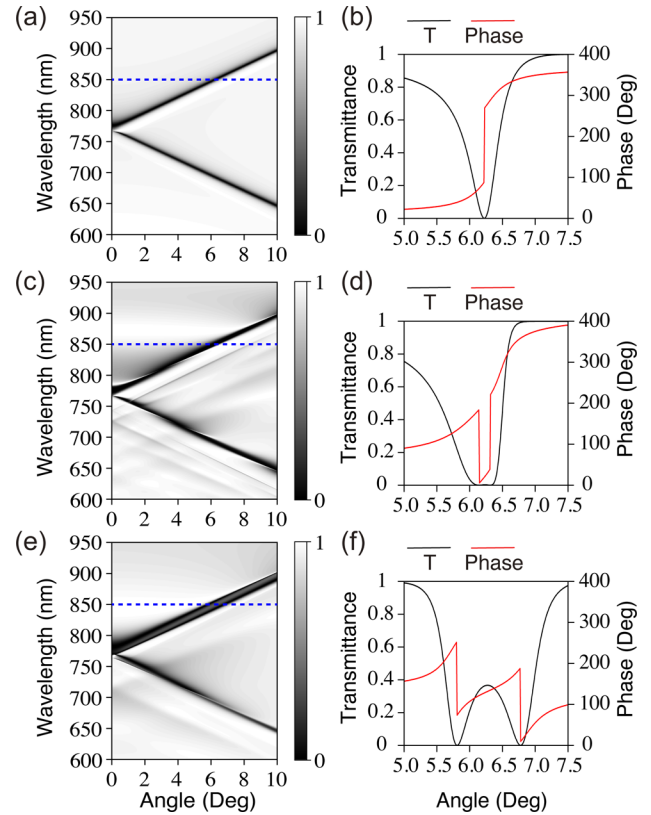

Fig. 2. Calculated TE transmittance spectra and the angular spectra with transmittance and transmissive phase of (a), (b) the single-layer grating, the coupled double-layer grating for (c), (d) $d = 2.0 \, \mu\mathrm{m}$, and (e), (f) $d = 0.8 \, \mu\mathrm{m}$.

between the two gratings when d is large. Dips still emerge in the transmissive spectra and the transmittance is low in the resonance region. Therefore, a smaller distance d is worth considering. Figures 2(e) and 2(f) show the calculated TE transmittance spectra and the angular spectra with transmittance and transmissive phase for $d = 0.8 \, \mu\mathrm{m}$ (1.6Λ). One can see that the gradient of the transmissive phase is preserved in the resonance region, which can be used to enhance the GH shift. Furthermore, a transmissive peak emerges within the transmissive dip, showing potential tunability. However, the zero points in the transmittance spectra are still present with the structure's mirror symmetry according to the middle horizontal plane. Further tuning with symmetry breaking is necessary for optimized transmissive GH shifts.

To further tune the coupling between the two gratings and introduce asymmetric perturbation, we varied the relative dislocation a of the two gratings for $d = 0.8 \, \mu\mathrm{m}$. The transmittance spectra and the angular spectra with transmittance and transmissive phase of the double-layer grating systems are calculated for $a = 0.05 \, \mu\mathrm{m}$ (0.1Λ) as shown in Figs. 3(a) and 3(b), $a = 0.15 \, \mu\mathrm{m}$ (0.3Λ) as shown in Figs. 3(c) and 3(d), and $a = 0.25 \, \mu\mathrm{m}$ (0.5Λ) as shown in Figs. 3(e) and 3(f) for TE polarization incidence at $\lambda = 850$ nm. One can see that with the increase of the relative dislocation, the transmittance of the double-layer grating continues to increase. Finally, the transmittance of the entire resonance region at $a = 0.5\Lambda$ is close to 1. At the same time, the variation of the transmitted phase does not depend significantly on the relative dislocation of the two
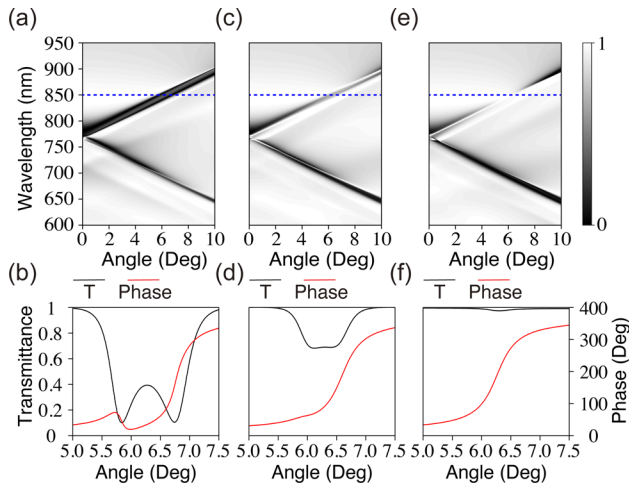
Fig. 3. Calculated TE transmittance spectra and the angular spectra with transmittance and transmissive phase of the coupled double-layer grating for (a), (b) $a = 0.05\,\mu m$, (c), (d) $a = 0.15\,\mu m$, and (e), (f) $a = 0.25\,\mu m$.

gratings. Taken together, the transmittance of the double-layer grating is close to 1, and the phase gradient is preserved with $d = 0.8\,\mu m$ and $a = 0.25\,\mu m$, as shown in Fig. 3(f), so it can be well used to enhance the transmitted optical GH shift.

To analyze the extreme transmissive of the double-layer grating system, we compare it to the anti-reflection coating, as shown in Fig. 4(a) inset. Anti-reflective coatings can achieve very high transmittance when the reflected waves are π radians out of phase difference [24]. The coupling of the double-layer grating is related to the distance and the relative dislocation between two identical gratings. The effect of this coupling is that after combining the transmissive phase of the upper grating and the reflection phase of the lower grating, an odd multiple of the π phase is generated to make the reflected light coherent and destructive. Therefore, a very high transmittance can be achieved. Figure 4(a) shows the angular spectra with the transmissive phase of the double-layer grating and twice that of the single grating, respectively. The solid black line represents two times the transmitted phase of the single-layer grating. The solid red line represents the transmitted phase of the double-layer grating.

The GH shift is not only related to the transmittance and the gradient of the transmissive phase but also related to the incident light, according to Eq. (1). Here, we choose a Gaussian beam with the wavelength 850 nm as the incident beam. Figure 3(f) shows that the GH shift reaches its maximum value at the incident angle $\theta = 6.25°$. Therefore, we take the incident angle as $6.25°$, which is also the center of the Gaussian beam in angular space. The maximum GH shift under the incident Gaussian beam can be obtained by Eq. (1). Figure 4(b) shows the relation between the maximum GH shift and the incident Gaussian beam waist. The transmitted GH shift of the double-layer grating increases with the beam waist radius. Note that the GH shift increases with a decreasing beam waist in total reflection. This difference is caused by the distribution of the phase gradient and the position of the incident angle.

To demonstrate the improvement of the GH shift efficiency of the double-layer grating system, the electric field distributions
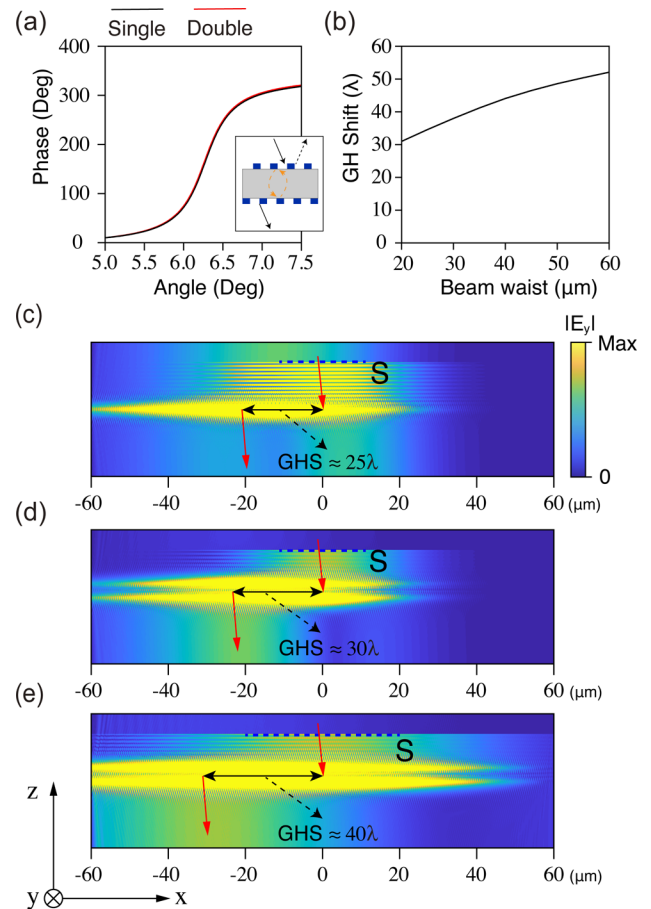

Fig. 4. (a) Angular spectra with transmissive phase. The inset indicates a schematic diagram of the coupling of the coupled double-layer grating. (b) Relation between the maximum GH shift and the incident Gaussian beam waist. (c) Simulated electric field distributions of the GH shift of the single grating. (d) Simulated electric field distributions of the GH shift of the double-layer grating. The waist radius of the Gaussian beam is 20 μm in panel (d) and 40 μm in panel (e).

of the GH shift of the single grating are simulated for comparison, as shown in Fig. 4(c). The waist radius of the Gaussian beam is 20 μm. The red arrows represent the central axes of the incident and transmitted beams. The dashed blue line S marks the center of the incident Gaussian beam. One can see that the simulated transmitted GH shift reaches 25 times the wavelength approaching the beam waist radius while the efficiency is low. Figure 4(d) shows the simulated electric field distributions of the GH shift of the double-layer grating with $d = 0.8\,\mu m$ and $a = 0.25\,\mu m$. The parameters of the incident light are the same as for the single grating. It can be seen that the transmitted GH shift of the double-layer grating system becomes larger, approaching 30 times the wavelength and 1.3 times the radius of the beam waist. Moreover, the efficiency of the GH shift has been greatly improved and almost all the beam is displaced. The transmitted GH shift will become more significant when the incident Gaussian beam waist radius increases to 40 μm. The simulated electric field distributions of the GH shift are shown in Fig. 4(e). The transmitted GH shift increases to approximately 40 times the wavelength. These results agree well with our previous assumptions.

In conclusion, we design a coupled double-layer grating system composed of two parallelly misaligned subwavelength dielectric gratings to achieve highly efficient large transmitted optical GH shifts. By changing the distance and the relative dislocation between two dielectric gratings, the coupling of the double-layer grating can be flexibly tuned, giving rise to electromagnetic responses. The transmittance can be close to 1 in the entire resonance region by adjusting the coupling. The gradient of the transmissive phase is also preserved. Therefore, the entire incident beam can be modulated and shifted. The efficient large transmitted GH shifts, approaching ~30 times the wavelength and 1.3 times the radius of the beam waist, can be observed directly. The efficient GH shifts in the coupled double-layer grating system can be used to design optical sensors, polarization beam splitters, and optical switches.

REFERENCES

1. F. Goos and H. Hänchen, Ann. Phys. **436**, 333 (1947).
2. K. Artmann, Ann. Phys. **437**, 87 (1948).
3. L.-G. Wang, H. Chen, and S.-Y. Zhu, Opt. Lett. **30**, 2936 (2005).
4. K. L. Tsakmakidis, A. D. Boardman, and O. Hess, Nature **450**, 397 (2007).
5. Y. Wan, Z. Zheng, W. Kong, X. Zhao, and J. Liu, IEEE Photonics J. **5**, 7200107 (2013).
6. X. Wang, C. Yin, J. Sun, J. Gao, M. Huang, and Z. Cao, J. Opt. **15**, 014007 (2013).
7. X. Li, P. Wang, F. Xing, X.-D. Chen, Z.-B. Liu, and J.-G. Tian, Opt. Lett. **39**, 5574 (2014).
8. X. Wang, M. Sang, W. Yuan, Y. Nie, and H. Luo, IEEE Photonics Technol. Lett. **28**, 264 (2015).
9. L. Han, J. Pan, C. Wu, K. Li, H. Ding, Q. Ji, M. Yang, J. Wang, H. Zhang, and T. Huang, Sensors **20**, 1028 (2020).
10. X. Wang, C. Yin, J. Sun, H. Li, Y. Wang, M. Ran, and Z. Cao, Opt. Express **21**, 13380 (2013).
11. R. Kaiser, Y. Levy, J. Fleming, S. Muniz, and V. S. Bagnato, Pure Appl. Opt. **5**, 891 (1996).
12. C.-F. Li, Phys. Rev. Lett. **91**, 133903 (2003).
13. W. J. Wild and C. L. Giles, Phys. Rev. A **25**, 2099 (1982).
14. J. Wen, J. Zhang, L.-G. Wang, and S.-Y. Zhu, J. Opt. Soc. Am. B **34**, 2310 (2017).
15. C.-F. Li and Q. Wang, Phys. Rev. E **69**, 055601 (2004).
16. F. Wu, J. Wu, Z. Guo, H. Jiang, Y. Sun, Y. Li, J. Ren, and H. Chen, Phys. Rev. Appl. **12**, 014028 (2019).
17. F. Wu, M. Luo, J. Wu, C. Fan, X. Qi, Y. Jian, D. Liu, S. Xiao, G. Chen, H. Jiang, Y. Sun, and H. Chen, Phys. Rev. A **104**, 023518 (2021).
18. C. Guo, H. Wang, and S. Fan, Optica **7**, 1133 (2020).
19. C. Huang, C. Zhang, S. Xiao, Y. Wang, Y. Fan, Y. Liu, N. Zhang, G. Qu, H. Ji, J. Han, L. Ge, Y. Kivshar, and Q. Song, Science **367**, 1018 (2020).
20. B. Wang, W. Liu, M. Zhao, J. Wang, Y. Zhang, A. Chen, F. Guan, X. Liu, L. Shi, and J. Zi, Nat. Photonics **14**, 623 (2020).
21. S. Du, W. Zhang, W. Liu, Y. Zhang, M. Zhao, and L. Shi, Nanophotonics **11**, 4531 (2022).
22. M. Moharam, D. A. Pommet, E. B. Grann, and T. Gaylord, J. Opt. Soc. Am. A **12**, 1077 (1995).
23. J. Wang, M. Zhao, W. Liu, F. Guan, X. Liu, L. Shi, C. T. Chan, and J. Zi, Nat. Commun. **12**, 6046 (2021).
24. H. K. Raut, V. A. Ganesh, A. S. Nair, and S. Ramakrishna, Energy Environ. Sci. **4**, 3779 (2011).